Hyper-Adamantane Networks

Mircea V. Diudea[a*] and Zahra Khalaj[b]

[a]Department of Chemistry, Faculty of Chemistry and Chemical Engineering
Arany Janos Str. 11, 400028, "Babes-Bolyai" University,Cluj, Romania, Europe
diudea@gmail.com
[b]Department of Physics, Shahr-e-Qods Branch, Islamic Azad University, Tehran, I. R. Iran
khalaj.z@gmail.com

Abstract. A hyper-adamantane, Hyp[ada.10](..).n is an ada.10 structure (the host structure), in which every vertex is replaced by a guest unit. Five triple periodic networks were designed by translating such hyper-adamantanes, along the orthogonal coordinate axes. Their repeating units were tested with respect to the rhombellanic character. Topological details on the concerned structures are given.

1. Introduction

In the recent years, crystal engineering and self-assembly processes have promoted new classes of finite and/or periodic nanostructures, with promising applications in material science and biosciences.

Based on Platonic and Archimedean solids, nano-sized spheroid architectures, with a variety of appropriate ligands have been synthesized [1–7]. The metals to join the ligands, include Pd2+ [3–6], Zn2+ [7], Cu2+ [8] etc.

The spherical structures, possessing large hollows, could be functionalized, both endo– and/or exohedrally. MOFs [9-12] are appreciated by their light structure, the voids inside being occupied by appropriate guests, or remaining empty. In the herein text, such light structures are termed "spongy" ones.

Adamantane, ada.10 molecule, was discovered by Landa (a Czech chemist) in 1933 in petrol [13]. The adamantane ada.10 is named tricyclo[3.3.1.13.7]decane, by the IUPAC nomenclature [14]. Hyper-clusters are polyhedral structures of which nodes are polyhedral structures (the same or different ones). Then a hyper-adamantane, e.g., Hyp[ada.10](ada.10).100 (Fig. 1, left) is an ada.10 structure (the host structure - in square brackets), in which every vertex is replaced by a guest unit (in this case, the same ada.10 – in round brackets).

Rhombellanes are structures with all rhomb/square rings, some of them forming local propellane substructures; they have been proposed by Diudea in 2017 [15]. Propellane was first synthesized in 1982 [16]; by IUPAC nomenclature, it is named tricyclo[1.1.1.01,3]pentane, a hydrocarbon with formula C5H6. Its reduced form, C5H8, or the bicyclo[1.1.1]pentane, has only rhomb/square rings; it can be represented as $K_{2.3}$ - the complete bipartite graph. The two bridge carbon atoms can be functionalized, e.g., by bromine or COOH, or even by repeating the $K_{2.3}$ motif, as in the staffane polymer [17,18].

A structure is a rhombellane if all the five conditions in Table 1 (left column) are obeyed [19-25]; these criteria have recently been reconsidered [24], in the view of accepting the presence of enlarged even-sized polygonal faces (with respect to the Omega criterion) and other than rbl.5 smallest tiles, thus defining related quasi-rhombellanes, as shown in Table 1 (right column).

Table 1. Criteria for rhombellanes and quasi-rhombelanes.

	Rhombellanes	Quasi-rhombellanes
1	All strong rings are r_4	*Rings are r_4 and/or even-sized rings/circuits.*
2	Vertex classes are non-connected inside a class	Vertex classes are non-connected inside a class
3	Omega polynomial has (at $r_{max}4$) a single term: $1x^\wedge e$	Omega polynomial has (at r_{max}) a single term: $1x^\wedge e$
4	Line graph has a Hamiltonian circuit	Line graph has a Hamiltonian circuit
5	There exist smallest units/tiles rbl.5 = $K_{2.3}$	*There are more smallest tiles:* rbl.5 = $K_{2.3}$ *and/or* ada.10, ...

Omega polynomial [26,27] $\Omega(x)$ was defined by Diudea (2006) on the ground of opposite edge strips, *ops*, in the graph. Denoting by *m*, the number of *ops* of length *s*, one can write: $\Omega(x) = \Sigma_s\, m_s X^s$. Its first derivative (in $x = 1$) counts the number of edges "*e*" in a graph: $\Omega`(1) = \Sigma_s\, sm_s = |E(G)| = e$. There are graphs with a single opposite edge stripe, which is a Hamiltonian circuit. For such graphs, Omega polynomial has a single term: $\Omega(x) = 1X^s$; $s = e$. This polynomial was implemented in the Nano Studio software package, developed at Topo Group Cluj, Romania [28]. It is computed within two ring size limits: $(r_{min}.r_{max})$ which define the maximal explored rings.

Finding vertex (subgraph) classes in a graph is related to Topological Symmetry. The vertex classes in the concerned structures are calculated as centrality classes, by using the Centrality index, C, developed at Topo Group Cluj [29]. It is calculated on layer/shell matrices [30,31], as:

$$C(\mathrm{LM} \setminus \mathrm{ShM})_i = \left[\sum_{k=1}^{ecc_i} \left([\mathrm{LM} \setminus \mathrm{ShM}]_{ik}^{2k} \right)^{1/(ecc_i)^2} \right]^{-1}; \quad C(\mathrm{LM} \setminus \mathrm{ShM}) = \sum_i C(\mathrm{LM} \setminus \mathrm{ShM})_i$$

This index allows to find the graph center and provides an ordering of vertices according to their centrality in the graph [32].

1. Results

1.1. Hyper-adamantane clusters

The hyper-adamantane, Hyp[ada.10](ada.10).100 (Fig. 1, left) was the first modeled [33] in a series of six hyper-adamantanes, Hyp[ada.10]()n, listed in Table 2, as follows: (i) (ada.10).100 (entry 1.2 – Fig. 1, left); (ii) (ada.1.10).88 (entry 1.4); (iii) (rh12.1.14).128 (entry 2.2); (iv) (rh24.1.26).248 (entry 3.2), (v) (rh6.1.8).68 (entry 4.2 – Fig. 1, right) and (vi) (CC.60).528 (entry 5.2). Table 2 lists also their topological substructure components and the corresponding values of Omega polynomial (see the next section).
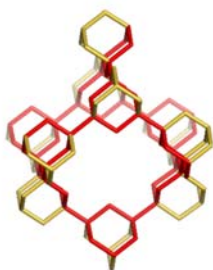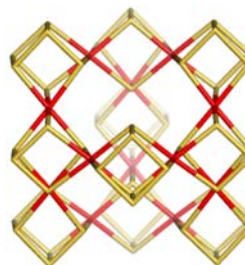
Hyp[ada.10](ada.10).100   Hyp[ada.10](rh6.1.8).68

Figure 1. Hyper-adamantane units

Table 2. Topology of hyper adamantane **Hyp[ada.10](..).n** units (italicized numbers count the maximum sized strong rings; bold-face numbers correspond to the values of r_{max}, giving the single term $1X^e$ in Omega polynomial).

	Cluster	v	e	cls	r_4	r_6	r_8	r_{12}	r_{14}	r_{16}	r_{18}	r_{20}	Omega polynomial
1	ada.10	10	12	2	0	4	**3**	0	0	0	*0*	**0**	$(6.6) = 4X^3$ $(6.8) = 1X^{12}$ ($r_{max\text{-}int}$)
1.1	(ada.10).60	60	78	5	0	24	18	0	0	0	*1*	**12**	$(6.6) = 6X^1+24X^3$ $(6.8) = 6X^1+6X^{12}$ $(6.20) = 1X^{78}$ (r_{max}+2)
1.2	(ada.10).100	100	132	9	0	40	30	0	0	0	*4*	**48**	$(6.6) = 12X^1 + 40X^3$ $(6.8) = 12X^1 + 10X^{12}$ $(6.20) = 1X^{132}$ (r_{max}+2)
1.3	(ada.1.10).54	54	72	5	0	24	18	*1*	**12**	72	280	780	$(6.6) = 24X^3$ $(6.8) = 6X^{12}$ $(6.14) = 1X^{72}$ (r_{max}+2)
1.4	(ada.1.10).88	88	120	7	0	40	30	*4*	48	0			$(6.6) = 40X^3$ $(6.8) = 10X^{12}$ $(6.12) = 1X^{120}$(r_{max})
2	rh12.14	14	24	2	12	0	**18**	*0*	0	0			$(4.4) = 4X^6$ $(4.8) = 1X^{24}$ ($r_{max\text{-}int}$)
2.1	(rh12.1.14).78	78	144	6	72	0	108	*1*	**12**	0			$(4.4) = 24X^6$ $(4.8) = 6X^{24}$ $(4.14) = 1X^{144}$ (r_{max}+2)
2.2	(rh12.1.14).128	128	240	9	120	0	180	*4*	50	0			$(4.4) = 40X^6$ $(4.8) = 10X^{24}$ $(4.12) = 1X^{240}$ (r_{max})
3	rh24.26	26	48	3	24	0	**15**	200	0	0			$(4.4) = 6X^8$ $(4.8) = 1X^{48}$ ($r_{max\text{-}int}$)
3.1	(rh24.1.26).150	150	288	11	144	0	90						$(4.4) = 36X^8$ $(4.8) = 6X^{48}$ $(4.14) = 6X^{48}$
3.2	(rh24.1.26).248	248	480	19	240	0	150						$(4.4) = 60X^8$ $(4.8) = 10X^{48}$ $(4.12) = 10X^{48}$
4	rh6.8	8	12	1	6	0	0	0					$(4.4) = 3X^4$
4.1	(rh6.1.8).42	42	72	4	36	0	0	64					$(4.4) = 18X^4$ $(4.8) = 18X^4$ $(4.14) = 4X^4+1X^{56}$
	(rh6.1.8).68	68	120	7	60	0	0	256					$(4.4) = 30X^4$ $(4.8) = 30X^4$

4.2											$(4.12) = 6X^4 + 1X^{96}$
5											$(6.6) = 24X^1 + 24X^2$ $(6.16) = 6X^4 + 6X^8$ $(6.18) = 1X^{72}$ $(r_{max}+2)$
	CC.60	60	72	3	0	8	0	0	0	*6*	**24**	
5.1											$(6.6) = 144X^1+126X^2$ $(6.16) = 36X^4+18X^8+3X^{36}$ $(6.18) = 1X^{396}$ $(r_{max}+2)$
	(CC.60).324	324	396	27	0	42	0	0	0	*36*	**144**	
5.2											$(6.6) = 240X^1 + 20X^2$ $(6.16) = 60X^4 + 30X^8 + 3X^{56}$ $(6.18) = 1X^{648}$ $(r_{max}+2)$
	(CC.60).528	528	648	31	0	68	0	0	0	*60*	**240**	

1.2. Hyper-adamantane networks

Excepting (ada.1.10).88, the other five hyper-adamantanes provided triple periodic networks in which the repeating units show the same vertex classes both as "selection" within the bulk network and as free/isolated adamantoid. Fig. 2 illustrates the nets corresponding to the clusters in Fig. 1 (as 2×2×2 domains) while Fig. 3 shows the network of Hyp[ada.10](CC.60).528) unit, (as 3×3×3 domains – see [25]), in two different projections. Vertex classes and the sequences of connectivity (LC) and rings around atoms (LR) for these networks are listed in Table 3.
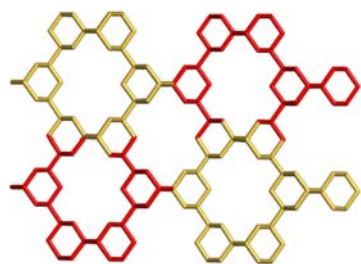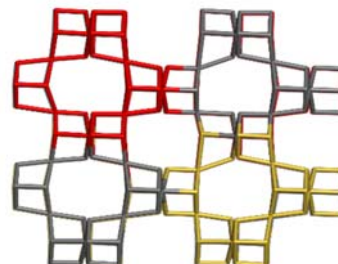
Hyp[ada.10](ada.10)-net (2×2×2)   Hyp[ada.10](rh6.1.8)-net (2×2×2)

Figure 2. Hyper-adamantane networks
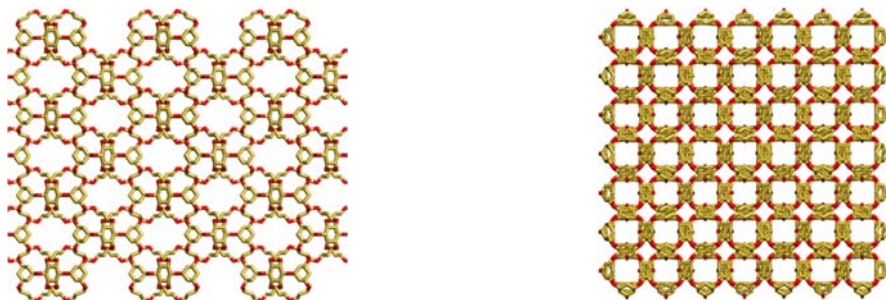
Figure 3. Etheric hyper-adamantane network (3x3x3); (unit: Hyp[ada.10](CC.60).528).

Table 3. Triple periodic network: unit/tile T; vertex connectivity classes; ring domain; population; degree; point symbol; LM sequence: connectivity (LC) and atom surrounding rings (LR).

Class	Network and vertex classes	LM
1	**Hyp[ada.10](ada.10) - net**	T_1: (Hyp[ada.10](ada.10)).100; (v = 100; e = 132; r_6 = 40; r_{18} = 4).
		ada.10 (v = 10; e = 12; r_6 = 4; r_8 = 3)
1.1	(6.6); {60}; | deg = 2 | 6^2	LC: {60}; 2.6.8.9.18.24.30.54.70.74.
	(6.18); {60}; | deg = 2 | 6^2.8^2.18^2	LR(4.4); {60}; 2.6.14.18.26.42.54.84.126.158.204.
		LR(4.12); {60}; 6.24.48.60.102.144.180.324.432.528.780.
1.2	(6.6); {40}; | deg = 4 | 6^3	LC: {40}; 4.6.9.15.18.27.45.54.75.105.
	(6.18); {40}; | deg = 4 | 6^3.8^3.18^6	LR(4.4); {40}; 3.9.15.24.33.45.72.99.135.198.231.
		LR(4.12); {40}; 12.30.54.90.108.162.270.324.486.738.756.
2	**(Hyp[ada.10](rh12.1.14)) - net**	T_1: (Hyp[ada.10](rh12.1.14)).128; (v = 128; e = 240; r_4 = 120).
		rh12.14 (v = 14; e = 24; r_4 = 12)
2.1	(4.4); 40 | deg = 3 | 4^3 (56)	LC: {40}; 3.6.12.19.39.63.114.148.207.252.
	(4.8); 40 | deg = 3 | 4^3.8^9	LR(4.4): {40}; 3.12.27.48.87.156.279.456.624.828.1062.
		LR(4.8): {40}; 12.48.108.192.348.624.1116.1824.2496.3312.4248.
2.2	(4.4); 60 | deg = 4 | 4^4 (60)	LC: {60}; 4.10.16.31.50.94.132.193.230.322.
	(4.8); 60 | deg = 4 | 4^4.8^12	LR(4.4): {60}; 4.18.40.72.124.222.376.564.772.966.1288.
		LR(4.8): {60}; 16.72.160.288.496.888.1504.2256.3088.3864.5152.
2.3	(4.4); 28 | deg = 6 | 4^6 (12)	LC: {28}; 6.12.24.38.72.108.168.198.276.330.
	(4.8); 28 | deg = 6 | 4^6.8^18	LR(4.4): {28}; 6.24.54.96.168.288.468.672.828.1104.1368.
		LR(4.8): {28}; 24.96.216.384.672.1152.1872.2688.3312.4416.5472.
3	**(Hyp[ada.10](rh24.1.26))- net**	T_1: (Hyp[ada.10](rh24.1.26)).248; (v = 248; e = 480; r_4 = 240).
		Rh24.26 (v = 26; e = 48; r_4 = 24)
3.1	**(4.4); 40 | deg = 3 | 4^3**	LC: {40}; 3.6.15.24.21.19.39.63.60.60.
	(4.8); 40 | deg = 3 | 4^3	LR(4.4): {40}; 3.12.30.60.84.84.96.156.219.240.300.
		LR(4.8): {40}; 3.27.60.135.204.189.186.351.519.540.600.
3.2	**(4.4); 180 | deg = 4 | 4^4**	
3.2.1	(4.8); 60 | deg = 4 | 4^4.8^10	LC: {60}; 4.8.14.17.18.24.36.50.60.74.
		LR(4.4): {60}; 4.16.34.56.64.72.102.144.192.240.312.

		LR(4.8): {60}; 14.36.74.126.134.162.222.324.432.540.672.
3.2.2	(4.8); 120 | deg = 4 | 4^4.8^5	LC: {120}; 4.9.14.17.20.27.37.48.62.84.
		LR(4.4): {120}; 4.17.36.55.68.81.108.147.192.252.336.
		LR(4.8): {120}; 9.37.81.125.153.171.243.327.432.552.756.
3.3	**(4.4); 28 | deg = 6 | 4^6**	LC: {28}; 6.12.12.12.24.38.36.36.72.114.
	(4.8); 28 | deg = 6 | 4^6	LR(4.4): {28}; 6.24.42.48.60.96.132.144.180.288.396.
		LR(4.8): {28}; 6.54.102.108.120.216.312.324.360.648.936.
4	**Hyp[ada.10](rh6.1.8) - net**	T_1: (Hyp[ada.10](rh6.1.8)).68; (v = 68; e = 120; r_4 = 60). rh6.8 (v = 8; e = 12; r_4 = 6)
4.1	(4.4); 40 | deg = 3 | 4^3 (4.12); 40 | deg = 3 | 4^3.12^192	LC: {40}; 3.12.10.33.30.88.60.150.102.250. LR(4.4); {40}; 3.18.36.60.99.180.264.360.450.612.750. LR(4.12); {40}; 195.1170.2340.3900.6435.11700.17160.23400.29250.39780.48750.
4.2	(4.4); 28 | deg = 6 | 4^6 (4.12); 28 | deg = 6 | 4^6.12^384	LC: {40}; 6.6.20.18.60.48.120.78.204.126. LR(4.4); {40}; 6.18.36.60.108.180.288.360.468.612.756. LR(4.12); {40}; 390.1170.2340.3900.7020.11700.18720.23400.30420.39780.49140.
5	**Hyp[ada.10](CC.60) - net**	T_1: (Hyp[ada.10](CC.60)); (v = 528; e = 648; r_6 = 68; r_{16} = 60). CC.60 (v = 60; e = 72; r_6 = 8; r_{16} = 6).
5.1	(6.16); {120}; deg = 2; 16^2.	LC: {120}; 2.4.3.5.9.12.18.22.26.22. LR: {120}; 2.6.8.11.18.28.36.44.58.57.69.
5.2	(6.16); {120}; deg = 2; 6.16.	LC: {120}; 2.4.6.8.9.13.20.20.24.28. LR: {120}; 2.7.12.18.20.24.39.52.58.68.82.
5.3	(6.16); {120}; deg = 3; 6.16^2.	LC: {120}; 3.3.5.6.9.15.19.24.23.29. LR: {120}; 3.6.10.14.20.30.40.51.54.66.77.
5.4	(6.16) ; {168}; deg = 3; 6.16^3.	LC: {168}; 3.5.7.9.12.14.16.20.23.28. LR: {168}; 4.10.15.18.22.29.36.50.66.70.71.

2. Discussion

The cluster Hyp[ada.10](ada.10) is the only one with no "coalesced" atoms in the units. In the other hyper-adamantanes, two neighbor units share an atom, i.e., the have a common coalesced atom; this is marked in the name of clusters by "1", between the number of rhombs and number of atoms, as in "rh6.1.8"; the simple "rh6.8" represents the shape of the cube, the mark "rh12.14" is the shape of rhombic dodecahedron. Observe that here one speaks rather about the "shapes" not the well-known geometrical structures; this is because, in this topological view, the angles and bond lengths are disregarded [34,35].

The hyper-adamantane networks show a single "hyper-tile" (marked T_1 in Table 3, the right column); this means that the "hyper-net" follows the type of primary net – the diamond *dia*-net, even the description of a tile (for the definition of "tile" see refs. [36,37]) could be here much complicated. In this view, we identified the single "hyper-tile" as the repeating hyper-adamantane Hyp[ada.10](..).n unit.

In adition to the vertex connectivity sequence, used in crystallography, and computed by Topo Group Cluj from the entries in the layer matrix of connectivity LC [29-31], our group proposed the use

of layer matrix of vertex surrounding rings [38] LR, the last one being a more powerfull topological tull in discriminating the crystal networks. Note that different LR count results (Table 3, the right column), function of the ring domain considered: $(r_{min}.r_{min})$ (corresponding to the ring symbol) or $(r_{min}.r)$, r-being a chosen value, working as a true "zoom" in separating the vertex classes.

With respect to the rhombelane character, the Omega polynomial criterion was investigated (see Table 2); the concerned clusters are rather *quasi*-rhombellanes, according to the criteria listed in Table 1, the right column. None of the discussed structures consist of $K_{2.3}$ smallest rhombellane. The next smallest tile in this respect is the adamantane ada.10, a tetrahedral tile (not a polyhedron), like $K_{2.3}$; among the discussed hyper-clusters, those "filled" by ada.10 are candidates to the status of quasi-rhombellanes (Table 2, entries 1.n). The disjoint vertex classes criterion seems to be fulfilled by virtue of repeating small fragments, like rhombs or hexagons, in conjunction with the symmetry of these fragments, in a fractalization process.

Finally, the Omega polynomial criterion, the single polynomial term, $1X^{\wedge}e$, is the most important among the five rhombellane criteria; is computed within two ring size limits, which define the maximal explored rings. In case of true rhombellanes, $(r_{min}.r_{max})$ is red $(r_4.r_4)$, (or simply (4.4) in the above tables) while in case of *quasi*-rhombellanes, r_{max} refers to the maximum sized strong rings in the graph; often, it is necessary r_{max+2}, to ensure the visiting of all edges in the graph when Omega polynomial is calculated; also is necessary to have a ring population larger than 1 (see Table 2, entries 1.1, 1.3, 2.1) or even more, in case of larger structures (see Table 2, entries 5,n). In case of the smallest units: ada.10; rh12.14 and rh24.26 (Table 2, entries 1, 2 and 3) $r_{max-int}$ refers to r_8, which is not a face but is a strong ring (i.e., a ring that is not the sum of other smaller rings).

The hyped-adamantane populated with (rh6.1.8), (see Table 2, entries 4) as well as the cube itself, do not show the $1X^{\wedge}e$ term; this is due probably to the fact that the line-graph of the cube (i.e., its medial, the octahedron) has all faces triangles; the same is for the "coalesced" cubes within these structures.

The enlargement of ring size to be visited within the "orthogonal cut process" of Omega polynomial is needed in respect of finding the single polynomial term, $1X^{\wedge}e$, that proves the existence of a Hamiltonian circuit in the "edge-graph", or "line-graph" of the parent concerned graph. No rational explanation was found so far for the r_{max} value needed to obey the $1X^{\wedge}e$ criterion. The empty cells of the Table 2 stand for the large circuits, computation of which is hard to be achieved, in more complex units and the corresponding hyper-adamantanes, also for the corresponding Omega polynomial. As above stressed, only the strong rings have to be considered in Omega polynomial count.

3. Conclusions

Hyper-clusters are polyhedral structures of which nodes are polyhedral structures, either the same or different ones. Then a hyper-adamantane, Hyp[ada.10](..).n is an ada.10 structure (the host structure), in which every vertex is replaced by a guest unit.

Five triple periodic networks were designed by translating, along the orthogonal coordinate axes. Their hyper-adamantane units were tested with respect to the rhombellanic character. Topological details on the concerned structures were given.

References

1. Sun, Q.F.; Iwasa, J.; Ogawa, D.; Ishido, Y.; Sato, S.; Ozeki, T.; Sei, Y.; Yamaguchi, K.; Fujita, M. Self−assembled M24L48 polyhedra and their sharp structural switch upon subtle ligand variation. *Science*, **2010**, *328*, 1144–1147.

2. Bunzen, J.; Iwasa, J.; Bonakdarzadeh, P.; Numata, E.; Rissanen, K.; Sato, S.; Fujita, M. Self-assembly of M24L48 polyhedra based on empirical prediction. *Angew. Chem. Int. Ed*. **2012**, *51*, 3161–3163.

3. Harris, K.; Fujita, D.; Fujita. M. Giant hollow MnL2n spherical complexes: Structure, functionalisation and applications.
Chem. Commun. **2013**, *49*, 6703–6712.

4. Fujita, D.; Ueda, Y.; Sato, S.; Mizuno, N.; Kumasaka, T.; Fujita, M. Self−assembly of tetravalent Goldberg polyhedra from 144 small components. *Nature*, **2016**, *540*, 563–566.

5. Fujita, D.; Ueda, Y.; Sato, S.; Yokoyama, H.; Mizuno, N.; Kumasaka, T.; Fujita, M. Self−assembly of M30L60 icosidodecahedron. *Chem.* **2016**, *1*, 91–101.

6. Suzuki, K.; Tominaga, M.; Kawano, M.; Fujita, M. Self−assembly of an M6L12 coordination cube. *Chem. Commun*.
2009, 1638–1640.

7. Lu, J.; Mondal, A.; Moulton, B.; Zaworotko, M. J. Polygons and faceted polyhedra and nanoporous networks.
Angew. Chem. Int. Ed. **2001**, *40*, 2113–2116.

8. Abrahams, B.F.; Egan, S.J.; Robson, R. A very large metallosupramolecular capsule with cube−like 43 topology assembled from twelve Cu(II) centers and eight tri−bidentate tri−anionic ligands derived from 2,4,6−triphenylazo−1,3,5−trihydroxybenzene. *J. Am. Chem. Soc*. **1999**, *121*, 3535–3536.

9. Fang, Z.; Bueken, B.; De Vos, D. E.; Fischer, R. A. Defect-Engineered Metal−Organic Frameworks. *Angew. Chem*., *Int. Ed*. **2015**, *54*, 7234−7254.

10. Öhrström, L. Framework chemistry transforming our perception of the solid state. *ACS Cent. Sci*. **2017**, *3*, 528−530. DOI: 10.1021/acscentsci.7b00230.

11. Qin, T.; Zhang, S.; Wang, Y.; Hou, T.; Zhu, D.; Jing, S. Three new topologically different metal-organic frameworks built from 3-nitro-4-(pyridin-4-yl)benzoic acid. *Acta Cryst*. **2019**, *C75*, 150-160; DOI:10.1107/S2053229618018211.

12. Liu, X.; Fu, B.; Li, L.; Jian, Y.-F.; Shu, S. Synthesis, crystal structure and photoluminescence of a three-dimensional zinc coordination compound with NBO-type topology. *Acta Cryst.* **2019**, *C75*, 277-282; doi.org/10.1107/S205322961900189X.

13. Landa, S.; Machácek, V. Sur l'adamantane, nouvel hydrocarbure extrait de naphte. *Collect. Czech. Chem. Commun*. **1933**, *5*, 1–5. doi:10.1135/cccc19330001.

14. Nomenclature of Organic Chemistry: IUPAC Recommendations and preferred names 2013 (Blue Book). Cambridge: The Royal Society of Chemistry, 2014. p. 169. Doi:10.1039/9781849733069-FP001. ISBN 978-0-85404-182-4.

15. Diudea, M. V. Rhombellanes – a new class of nanostructures. Int. Conf. "Bio-Nano-Math-Chem" 2017, Cluj, Romania.

16. Wiberg, K. B.; Walker, F. H. [1.1.1]propellane. *J. Am. Chem. Soc*. **1982**, *104*, 5239–5240.

17. Kazynsky, P.; Michl, J. Staffanes: a molecular−size tinkertoy construction set for nanotechnology. Preparation of end−
functionalized telomers and a polymer of [1.1.1]propellane. *J. Am. Chem. Soc.* **1988**, *110*, 5225–5226.

18. Dilmaç, A.; Spuling, E.; de Meijere, A.; Bräse, S. Propellanes-from a chemical curiosity to "explosive" materials and natural
products. *Angew. Chem., Int. Ed*. **2017**, *56*, 5684−5718.

19. Diudea, M. V. Hypercube related polytopes. *Iranian J. Math. Chem*. **2018**, *9*, 1-8.

20. Diudea, M. V. Rhombellanic crystals and quasicrystals. *Iranian J. Math. Chem*. **2018**, *9*, 167-178.

21. Diudea, M. V. Rhombellanic diamond. *Fullerenes, Nanotubes and Carbon Nanomaterials*, **2018**, Doi: 10.1080/1536383X.2018. 1524375.

22. Diudea, M. V.; Nagy, C. L. Rhombellane space filling, *J. Math. Chem.* **2018**, Doi.org/10.1007/s10910-018-0959-5.

23. Diudea, M. V. Cube-Rhombellane: from Graph to Molecule, *Int. J. Chem. Model,* **2018**, *9* (2-3), 97-103.
24. Diudea, M. V. Rhombellanes and quasi-rhombellanes. *J. Eur. Soc. Math. Chem.* **2018**, *1* (1), 1.
25. Diudea, M. V. Hyper-structural ethers. *J. Eur. Soc. Math. Chem.* **2018**, *1* (1), 6.
26. Diudea, M. V. Omega polynomial, *Carpath. J. Math.*, **2006**, *22*, 43–47.
27. Diudea, M. V.; Klavžar, S. Omega polynomial revisited, *Acta Chem. Sloven.* **2010**, *57*, 565–570.
28. Nagy, C.L.; Diudea, M.V. Nano−studio software, Babes−Bolyai University, Cluj, Romania, 2009.
29. Diudea, M. V.; Ursu, O. Layer matrices and distance property descriptors. Indian J. Chem. A, 2003, 42, 1283-1294.
30. Diudea, M. V. Layer matrices in molecular graphs. J. Chem. Inf. Comput. Sci. 1994, 34, 1064-1071.
31. Diudea, M. V.; Topan, M.; Graovac, A. Molecular topology. 17. Layer matrixes of walk degrees. J. Chem. Inf. Comput. Sci. 1994, 34, 1072-1078.
32. Diudea, M. V. *Multi-shell polyhedral clusters*. Springer International Publishing, AG 2018.
33. Diudea, M. V.; Medeleanu, M.; Khalaj, Z.; Ashrafi, A. R. Spongy diamond. *Iranian J. Math. Chem.* **2019,** *10*(1), 1-9.
34. Schulte, E. Regular incidence-polytopes with Euclidean or toroidal faces and vertex-figures. *J. Combin. Theory, Series A*, **1985**, *40*(2): 305–330.
35. Schulte, E. Polyhedra, complexes, nets and symmetry. *Acta Cryst.* **2014**, *A70*, 203-216.
36. Blatov, V. A.; Delgado Friedrichs, O.; O'Keeffe, M.; Proserpio, D. M. Three-periodic nets and tilings: natural tilings for nets. Acta Cryst. 2007, A63, 418-425.
37. Blatov, V. A.; O'Keeffe, M.; Proserpio, D. M. Vertex-, face-, point-, Schläfli-, and Delaney-symbols in nets, polyhedra and tilings: recommended terminology. Cryst. Eng. Comm. 2010, 12, 44-48.
38. Nagy, C. L.; Diudea, M. V. Ring signature index. *MATCH Commun. Math. Comput. Chem.* **2017**, 77(2), 479-492.